Research Article Vol. 28, No. 1 / 6 January 2020 / Optics Express 288
Optics EXPRESS

Generation of lossy mode resonances with different nanocoatings deposited on coverslips

OMAR FUENTES,[1,2] JAVIER GOICOECHEA,[1,3] JESUS M. CORRES,[1,3] IGNACIO DEL VILLAR,[1,3,*] ARITZ OZCARIZ,[1,3] AND IGNACIO R. MATIAS[1,3]

[1]Institute of Smart Cities (ISC), Public University of Navarra, 31006 Pamplona, Spain
[2]Department of Telecommunications and Electronics, Pinar del Río University, Pinar del Río CP 20100, Cuba
[3]Electrical and Electronic Engineering Department, Public University of Navarra, 31006 Pamplona, Spain
*ignacio.delvillar@unavarra.es

Abstract: The generation of lossy mode resonances (LMRs) with a setup based on lateral incidence of light in coverslips is a simple platform that can be used for sensing. Here the versatility of this platform is proved by studying the deposition of different coating materials. The devices were characterized with both SEM and AFM microscopy, as well as ellipsometry, which allowed obtaining the main parameters of the coatings (thickness, refractive index and extinction coefficient) and relating them with the different sensitivities to refractive index attained with each material. In this way it was possible to confirm and complete the basic rules observed with lossy mode resonance based optical fiber sensors towards the design of simpler and more compact applications in domains such as chemical sensors or biosensors.

1. Introduction

The generation of lossy mode resonances (LMR) with polymers and metallic oxides deposited on optical fiber is a topic that has attracted much interest during the last decade thanks to the properties it presents: ability to generate the resonance both for TE and TM polarized light, possibility to obtain multiple resonances and the capability to tune its position in the optical spectrum [1–7], which has resulted in many publications where LMR based optical fiber sensors are used for detecting refractive index variation [8–11], humidity [12], pH [3], chemical or biological species [6,13], gases [14] or even voltage [15,16].

The idea of a thin-film inducing attenuation maxima in the transmission spectrum was first proposed in the domain of semiconductor waveguides [17–19]. After that, a practical optical fiber sensor configuration where LMRs are tracked as a function of wavelength was demonstrated [8] and the correlation between theory and experiments was stablished in 2010 [2].

The basic rules that determine the sensitivity of the device can be summarized in tracking the first LMR (i.e. the LMR that is generated with a thinner coating), to operate with substrate and outer medium refractive indices that are as similar to each other as possible, and to use a nanocoating material whose refractive index is as high as possible [7,20]. Another important question is the width of the resonance [21], which can be greatly reduced by using a configuration where a single mode is transmitted and the contribution in the optical spectrum of TM and TE resonance can be separated. In structures with cylindrical symmetry the separation of both components is not evident, and both TE and TM resonances can be distinguished in the same spectrum only when the nanocoating refractive index is very high, as it was the case with In_2O_3 deposited with dip coating technique, for example [22]. However, with a D-shaped fiber it was possible to solve both issues: the device is single-moded and its non-cylindrical symmetry allows showing either the TE or the TM resonance in the spectrum. To this purpose, it is necessary to

#371346 https://doi.org/10.1364/OE.28.000288
Journal © 2020 Received 1 Jul 2019; revised 15 Sep 2019; accepted 10 Nov 2019; published 2 Jan 2020

Optics EXPRESS

use in-line polarizer and a polarization controller that permits to control the polarization in a standard single-mode fiber [10], or to employ a side-polished polarization maintaining fiber [8].

More recently, it has been demonstrated that it is possible to generate lossy mode resonances by lateral light incidence in nanocoated planar waveguides [23,24]. There are several advantages in using a planar structure compared to optical fiber. The first one is precisely related to the polarization. D-shaped fiber, the best optical fiber structure for development of lossy mode resonance sensors, presents a higher complexity in controlling the polarization in each experiment compared to simply orienting the polarization of a polarizer vertically or horizontally [24]. In addition, the planar structure is a more robust platform than optical fiber and the need of splices is avoided. Therefore, the slab waveguide setup is easier to handle. Another important advantage with the planar waveguide is that it is possible to operate in a wide spectrum with either the TE or the TM resonance separately, something that has been proved only in the case of optical fiber with SMF D-shaped fiber, which limits greatly the range of operation of the device. In addition, the waveguide can be deposited on both sides, allowing to obtain easily a two parameter sensor or even a two channel microfluidic system that is easier to introduce in a flow cell, because unlike for optical fibers, it is not necessary to glue to fiber in order to avoid bending during the flow of the liquid, while the volume of the inner cavity of the flow cell can be reduced a lot since the inherent higher robustness of the slab waveguide compared to optical fiber prevents it from attaching the walls of the inner cavity of the flow cell. Furthermore, taking into account its simplest configuration, robustness, etc., its transfer to the industry seems more straightforward than its fiber optic counterpart. For all this reasons, and in view of the results achieved already with optical fiber [25], it is a good platform for development of chemical and biological applications.

In this work, we compare different materials with the purpose of testing if the sensitivity can be improved by increasing the coating refractive index [7]. To this purpose, tin oxide (SnO_2), copper oxide (CuO) and indium tin oxide (ITO) were analyzed as nanocoating materials.

2. Materials and methods

The experimental setup is illustrated in Fig. 1. The light source used was an ASBN-W tungsten-halogen broadband from Spectral Products Inc. (Putnam, FL, USA). Light was launched into a multimode optical fiber from Ocean Optics (200/225 µm of core/cladding diameter). This fiber was placed in front of a visible linear polarizer from Thorlabs (LPVIS050). A planar waveguide was positioned after the polarizer. The output light of the waveguide was collected by another multimode optical fiber whose end was connected to an HR4000 spectrometer (OceanOptics Inc., Largo, FL, USA). As planar waveguides we used RS France microscope coverslips (18×18×0.15 mm) made of soda lime glass [26]. The planar waveguide was coated with three different materials (SnO_2, CuO and ITO) and placed on poly(methyl methacrylate) (PMMA) substrate. PMMA is a good material because its refractive index is slightly lower than the soda lime coverslip [27], which permits to guide light through the coverslip.

The setup without the polarizer was placed in a DC sputtering machine (K675XD from Quorum Technologies, Ltd.) in order to observe the evolution of the optical spectrum during the deposition (to this purpose the pigtails connected to the light source and the detector enter the sputtering machine via a feedthrough). The reason why the polarizer is not introduced is because it can be damaged due to the deposition, while it is possible to observe the generation of the LMRs with unpolarized light [23].

In addition, different targets (all of them of 57 mm in diameter and 3 mm in thickness) were used for coating with SnO_2, CuO and ITO. CuO and ITO targets were purchased from ZhongNuo Advanced Material Technology Co, whereas the SnO_2 target was from Plasmaterials, Inc.

The parameters used for the DC sputtering deposition were: the argon partial pressure was of 7×10^{-2} mbar for all the targets while the intensity was 150 mA for ITO, 80 mA for SnO_2 and for CuO 70 mA.

Optics EXPRESS

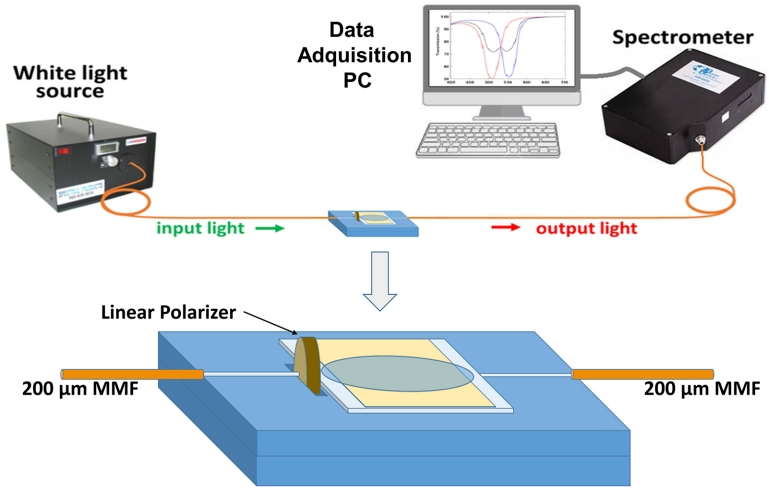

Fig. 1. Experimental setup used for the characterization as a refractometer of coverlips coated with different materials. The system allows controlling the polarization of light in order to visualize the TE or the TM resonance in the optical spectrum.

In all cases the coverslip was positioned at a distance of 7 cm from the target and the optical spectra was monitored continuously during the deposition process. During the deposition process, a mask was used to avoid material deposition on the lateral surfaces of the coverslip.

The nanocoatings where characterized with AFM microscopy (Bruker Innova with RTESPA probes in tapping mode) and with a field emission scanning electron microscope (model UltraPlus FESEM from Carl Zeiss Inc.) with an in-lens detector at 3 kV and an aperture diameter of 30 µm). Both measurements permitted to estimate the coating thickness. In addition, the coatings were also characterized with an ellipsometer UVISEL 2 from Horiba, with spectral range of 0.6−6.5 eV (190−2100 nm), an angle of incidence of 70°, a spot size of 1 mm and software DeltaPsi2TM (from Horiba Scientific Thin Film Division). With this instrument is was also possible to obtain the dispersion curves (the refractive index and the extinction coefficient) of the three materials.

3. Results

As indicated in section 2, the coverslips were deposited with a DC sputtering machine and the evolution of the optical spectrum was continuously monitored. The deposition process was stopped in all cases when an attenuation corresponding to the first LMR started to be observed in the optical spectrum. In this sense, Fig. 2 shows the spectrum after the deposition process.

There, it is interesting to observe that, for the SnO_2 coating, the first TE LMR is present at about 570 nm as a side lobe and the TM LMR is visible at a shorter wavelength (450 nm), as observed in other works [28] (the presence of both TE and TM LMRs is explained by the fact that in the sputtering machine the polarizer was not used due to the difficulty of protecting it during deposition). With respect to the CuO spectrum, the resonance is wider. This is explained because the TE and the TM resonances are deeper and they overlap each other [20]. Finally, for the ITO coating there is a shallow and difficult to distinguish TE resonance located at about 630 nm, whereas the TM LMR is easier to visualize at about 400 nm.

As indicated in section 2, the coverslips were also characterized with the aid of an SEM and an AFM microscope. SEM images are shown in Fig. 3, where it can be seen that the thickness of CuO is 50 nm, thinner than the 70 nm and the 83 nm thickness of ITO and SnO_2 coatings, respectively.

Optics EXPRESS

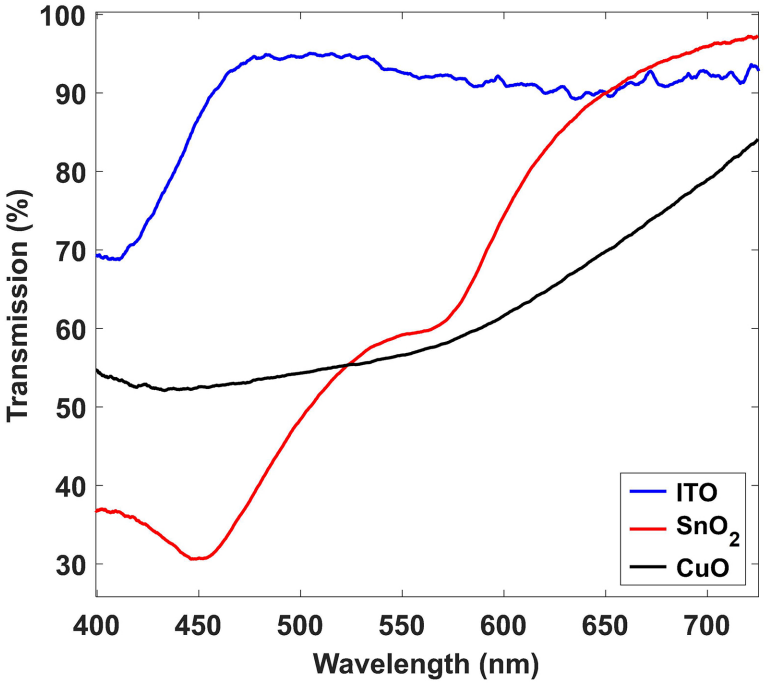

Fig. 2. Optical spectra after a 3 minute deposition of three different materials (ITO, SnO_2, CuO) with a DC sputtering machine.

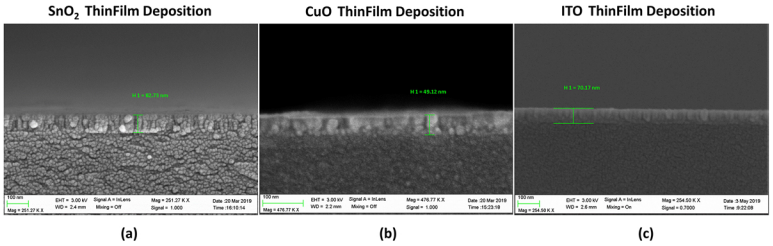

Fig. 3. SEM microscope images showing the thickness of the different materials deposited on the coverslips coated with (a) 82.73 nm SnO_2 thin-film; (b) 49.12 nm CuO thin-film; (c) 70.17 nm ITO thin-film.

Optics EXPRESS

The thickness of the sputtered coatings was characterized using Atomic Force Microscopy (AFM) (Bruker Innova, 100 µm scanner) in tapping mode with RTESPA-150 AFM probes (30 µm scans using a scanning frequency of 0.5 Hz). The substrates were protected with a mask during the sputtering process so that it was possible to measure the step height from the substrate to the coating surface. For each sample, AFM measurements were performed 5 times in different zones in order to obtain the mean value of the film thickness and its standard deviation. The roughness of the surfaces was estimated using the root mean square roughness (rms) in a homogenous area of the coating avoiding strange particles or measurement artifacts.

The results obtained AFM microscope in Fig. 4 present a general agreement with the SEM results previously shown in Fig. 3.

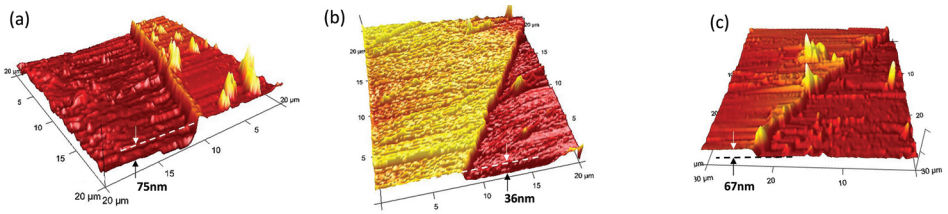

(d)

	Thickness (nm)
SnO_2	75 ± 4,7
CuO	36 ± 2
ITO	67,3 ± 1,5

Fig. 4. AFM microscope images showing the thickness and roughness of the different materials deposited on the coverslips: (a) SnO_2; (b) CuO; (c) ITO.

Finally, the dispersion curves of the nanocoatings were obtained with the aid of the ellipsometer described in section 2. In Fig. 5, it is interesting to observe that the refractive index of the materials in the range of 400 to 1000 nm (the region where we will characterize the devices as a refractometer) ranges from 1.85 to 1.95 in the case of SnO_2, from 2.15 and 2.35 in the case of CuO and from 1.9 to 2.1 in the case of ITO.

This values agree well with the coating thicknesses presented in Fig. 3 and Fig. 4, because it is well known that the sensitivity to thickness of LMRs (i.e. resonance wavelength shift per nm thickness increase), depends on the coating refractive index [7,20], and consequently the LMR corresponding to the material with a higher refractive index should be obtained with a thinner coating. In this sense, the CuO is the material with a higher refractive index and it presents the lowest thickness. Regarding the second material with a higher refractive index, ITO, its coating is the second one in order of thickness, whereas the material with the lowest refractive index, SnO_2, presents the thicker coating. These results contradict the results obtained in [13], where SnO_2 presents a higher refractive index than ITO. However, it must be pointed out that in that publication the SnO_2 target was acquired from ZhongNuo Advanced Material Technology Co, while the target for sputtering used here was produced by Plasmaterials, with a not so dark colour, indicating that is was not as oxygen depleted as the target of ZhongNuo.

In addition, the high refractive index of copper oxide agrees well with the literature, where it is stated that copper oxide, in its different forms (CuO and Cu_2O), presents a very high refractive index [29]. In addition, the big difference among CuO and both ITO and SnO_2, it that ITO is actually indium tin oxide. Therefore, it seems logical that CuO presents a quite different dispersion curve.

According to the design rules for LMR based sensors, a higher coating refractive index also induces a higher refractive index sensitivity [20,30].

Optics EXPRESS

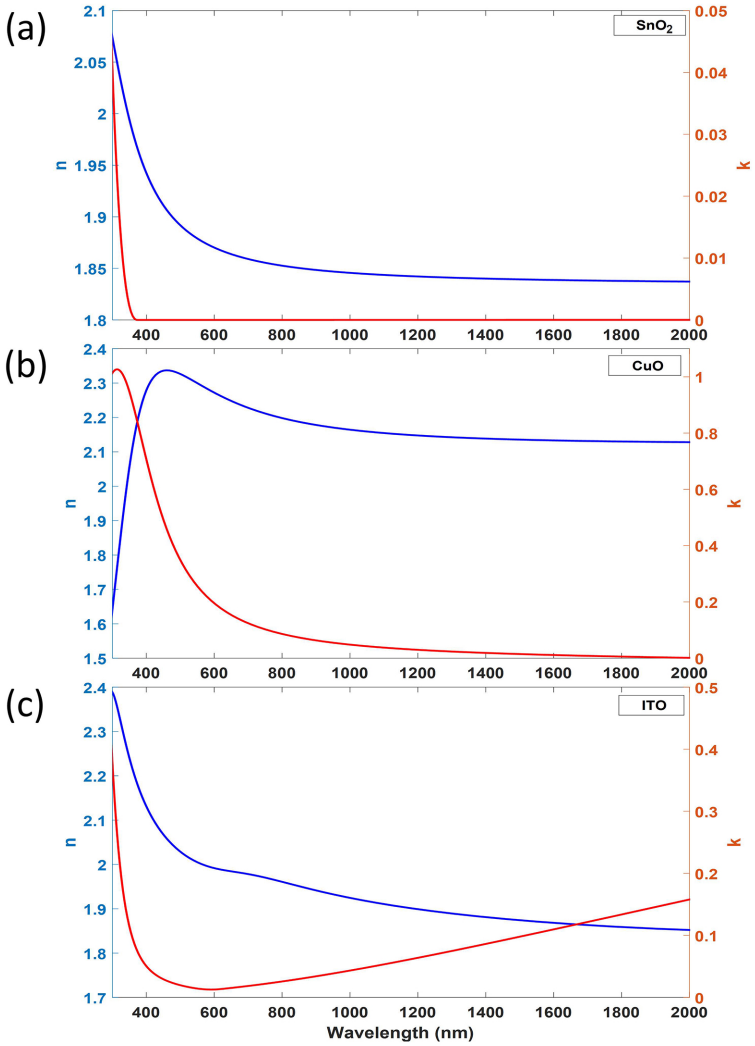

Fig. 5. Refractive index (n) and extinction coefficient (k) of: (a) SnO_2 thin-film; (b) CuO thin-film; (c) ITO thin-film.

In order to check the validity of this assertion, the coated region was sequentially submerged in several glycerine solutions (Panreac Technical Grade) and the refractive index was measured with the commercial refractometer (Mettler Toledo Refracto 30GS). In Figs. 6, 7 and 8, it is possible to observe the wavelength shift of the TE and TM resonance to the infrared obtained with SnO_2, CuO and ITO coated coverslips with the increase of the refractive index.

For a more accurate comparison, in Fig. 9 the LMR wavelength shift obtained with the three materials is shown as a function of refractive index.

The first comparison will be between CuO and ITO sensors, whose resonances in Fig. 9 are located at similar wavelengths, avoiding in this way the influence of wavelength. Here it is important to highlight that, due to the higher sensitivity of CuO to the coating thickness, it is not possible to track with the same coverslip the refractive index both with TE and TM polarization because the resonances corresponding to these polarizations are far apart and do not fit in the range of the spectrometer.

Optics EXPRESS

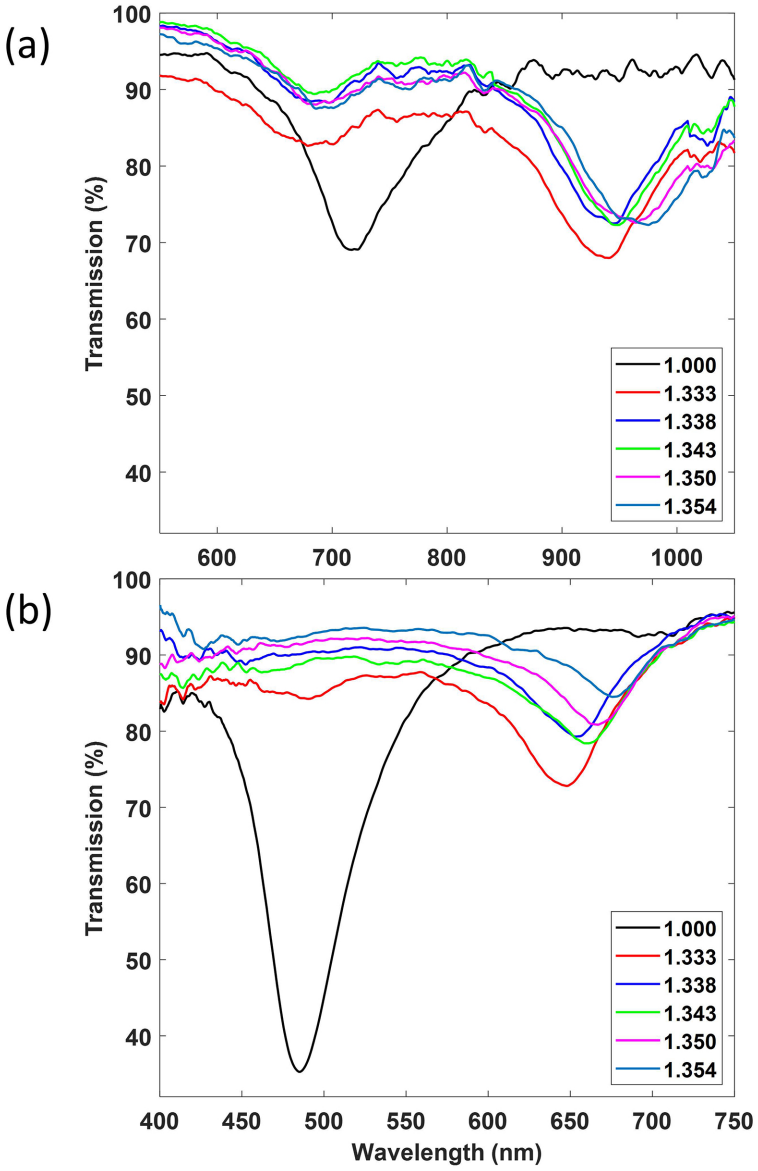

Fig. 6. Transmission spectra of SnO_2 coated coverslip surrounded by different refractive indices: (a) TE polarization, (b) TM polarization.

In these sense, the results for the TE resonance were obtained with the coating thickness presented in Figs. 3 and 4. However, the TM resonance was not visible with this thickness (the higher separation of TE and TM resonance compared to ITO and SnO_2 confirms the idea of the higher sensitivity to the coating thickness). That is why it was necessary to fabricate a new device with a thicker CuO nanocoating. If we compare CuO with ITO, the first one presents a higher sensitivity than ITO. In the TE case, where the CuO resonance is located at a shorter wavelength than the ITO resonance, the sensitivity of CuO is 10% better than ITO, while in the TM case, where the CuO resonance is located at a longer wavelength, a 33% improvement is observed. As a result, on average a 21.5% improvement is obtained.

Optics EXPRESS

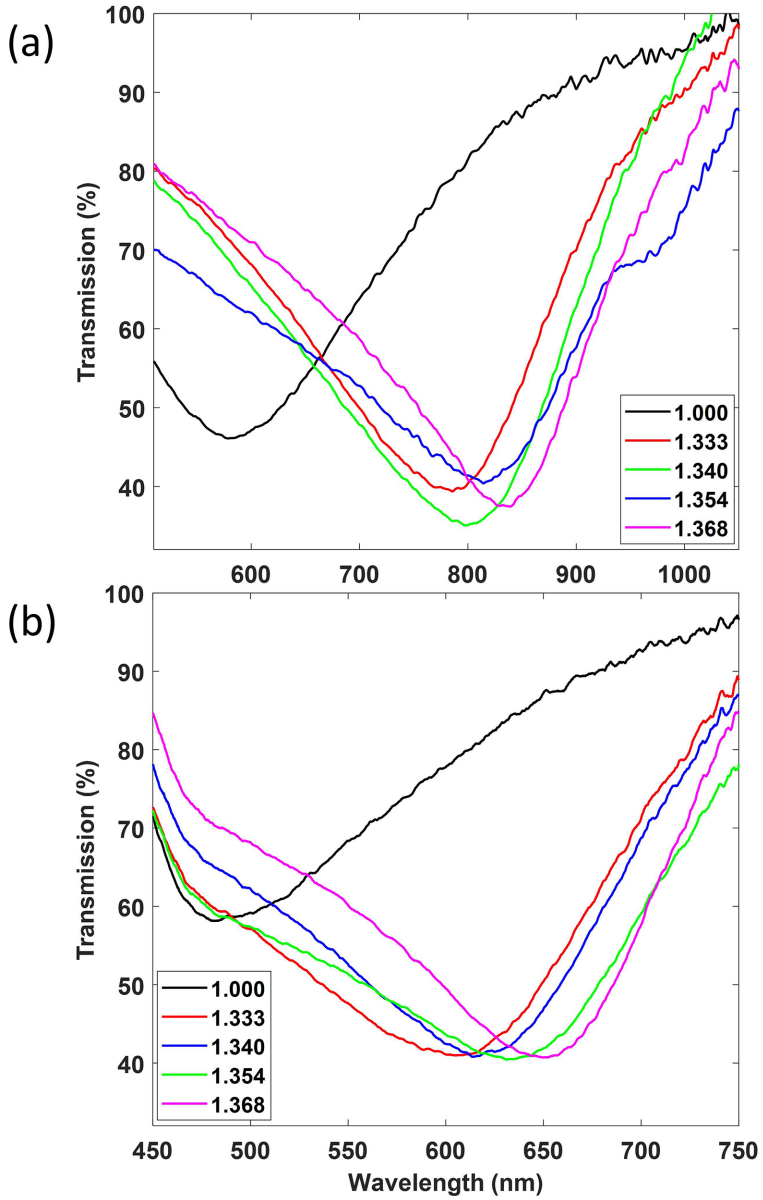

Fig. 7. Transmission spectra of CuO coated coverslip surrounded by different refractive indices: (a) TE polarization, (b) TM polarization.

If we consider that in Fig. 5 the refractive index of CuO is 2.15-2.35 (average 2.2), while the refractive index of ITO is located between 1.9 and 2.1 (average 2), there is on average a refractive index difference of 0.2 refractive index units, and according to [20] the sensitivity increase observed in an LMR located at 600 nm by comparing two coatings of refractive index 1.8 and 2 should be 10%. This value is lower than the experimental one but in both cases it indicates that the sensitivity improvement attained by increasing the coating refractive index is not so critical.

Regarding ITO and SnO_2, in principle it should be difficult to observe some differences because the coating refractive index difference is not so great (approximately 0.1 refractive index units)

Optics EXPRESS

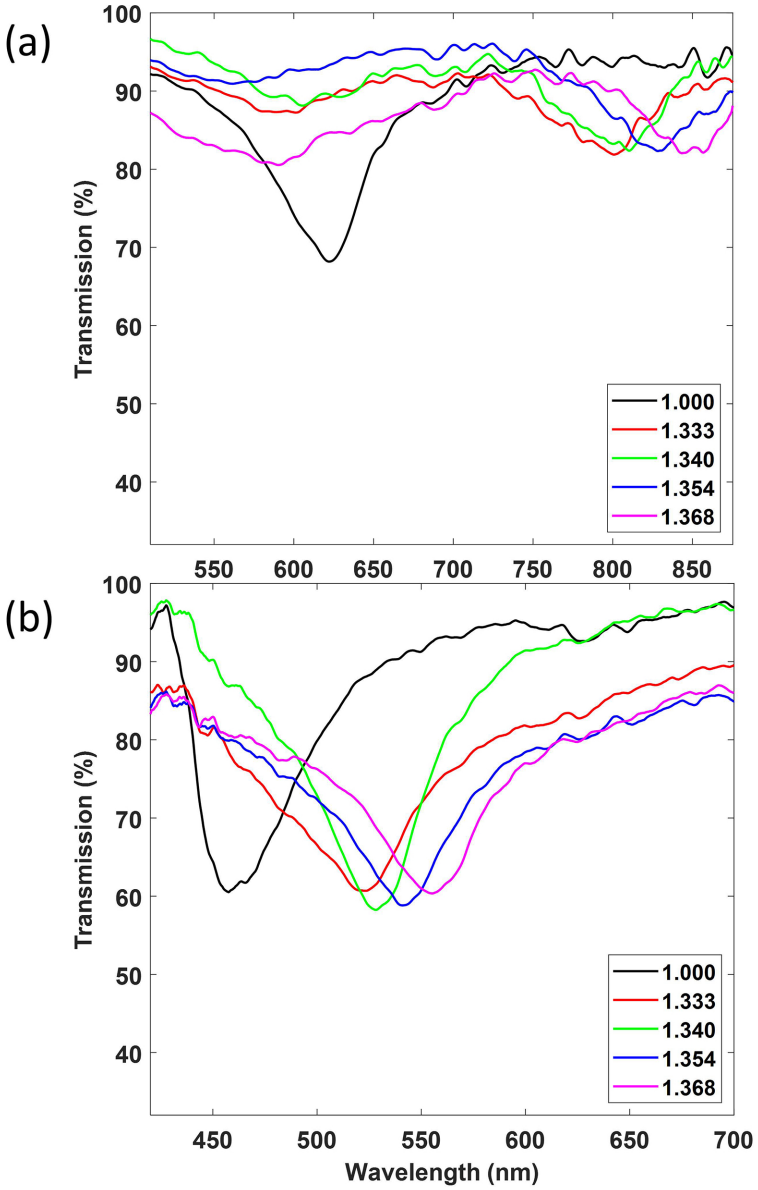

Fig. 8. Transmission spectra of ITO coated coverslip surrounded by different refractive indices: (a) TE polarization, (b) TM polarization.

and the required coating thickness to position the LMR in the visible wavelength range only differs by 10 nm. However, the LMRs in Fig. 9 are widely separated in wavelength. The TE resonance of SnO_2 is located in water at a higher wavelength compared to the TE resonance of ITO in water (935 vs 780 nm), whereas the TM resonance of SnO_2 is located in water at a higher wavelength compared to the TM resonance of ITO in water (650 vs 520 nm). This is what causes that, unexpectedly, the sensitivity with SnO_2 is higher than that of ITO (the increase in refractive index sensitivity as a function of wavelength is a typical phenomenon in optical sensors [1,31]).

Optics EXPRESS

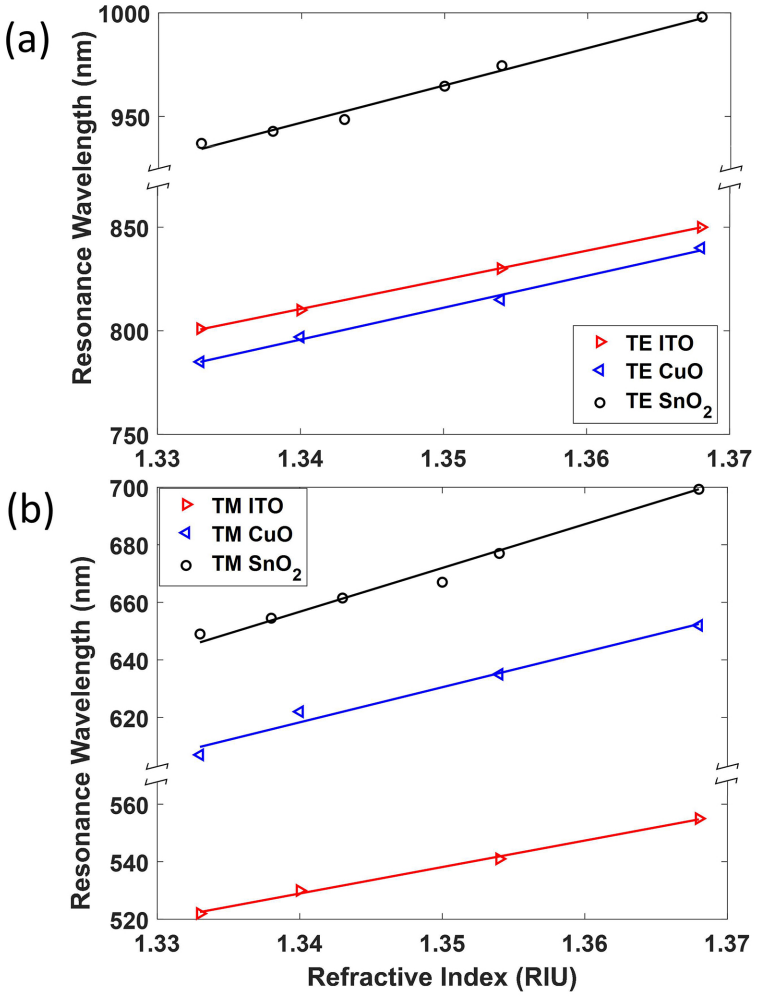

Fig. 9. Representation of the central wavelength of the resonances as a function of the surrounding refractive index (SRI) in different materials (SnO_2, CuO, and ITO) and polarization: (a) TE Polarization and (b) TM Polarization.

In [20] the main design rules of lossy mode resonance sensors were obtained with coated optical fiber by comparing two materials whose real part of the refractive index was very different: one of them was PAH/PAA, with refractive index 1.5, and the other titanium oxide, with refractive index 2. With such a big difference it was easy to extract the conclusion that the sensitivity is increased by increasing the real part of the refractive index. That is why focus has been centered during the last years in finding materials with high refractive index. However, it was also theoretically predicted that the sensitivity does not increase constantly as a function of refractive index [20], something that has been confirmed theoretically here: though there is an important difference in refractive index among ITO, SnO_2 and CuO, the sensitivity is not greatly enhanced as function of refractive index because all of them have a refractive index that is greater than 1.8, while there is another parameter, wavelength, that plays a major role compared to refractive index, i.e. the central wavelength of the resonance.

A good way to avoid the influence of the wavelength on the sensitivity results could be to use the normalized resonance wavelength [32]. However, this method will only mitigate the influence

Optics EXPRESS

of wavelength, since the dependence on wavelength is not just proportional to wavelength. In lossy mode resonance sensors this effect is specially dramatic; it has been observed with the same resonance positioned at short wavelengths (600-700 nm) and at long wavelengths (1300-1500 nm) that the sensitivity is increased by a factor of more than 3 [1].

As a result, Fig. 9 and Table 1 also show that the sensitivity of the SnO_2 sensor is even higher than the sensitivity of the CuO sensor (24% increase compared to CuO in TM polarization and 17% in TE polarization), and in this case it is not only the question that SnO_2 presents a slightly lower refractive index; this time CuO is 0.35 higher than SnO_2 on average.

Table 1. Sensitivities to refractive index with different materials

Material	TE Sensitivity (nm/RIU)	TM Sensitivity (nm/RIU)
SnO_2	1800	1510
CuO	1537	1220
ITO	1405	920

Therefore, though the rule of increasing the sensitivity to refractive index by increasing the coating refractive index remains valid, its influence is not so appreciable and, as we have observed, the wavelength plays a major role.

There is an additional element that has been barely addressed in the literature of LMRs and which distorts the conclusions about sensitivity with different materials. In [20], for the sake of simplicity, materials with a very flat dispersion were analyzed (i.e. the refractive index is nearly constant in the wavelength range analyzed). However, the materials analyzed here present non-negligible dispersion in the real part of the refractive index. In this sense, it is important to remark that a refractive index decrease as a function of wavelength leads to a decrease in sensitivity, because the decrease in refractive index reduces the wavelength shift of the LMR [2], while a refractive index increase as a function of wavelength should lead to a sensitivity increase. This idea is quite difficult to prove experimentally, because models obtained with ellipsometers are not exact measurements, but the unexpected higher sensitivity observed with SnO_2 compared to ITO at wavelengths above 1000 nm [33], suggests that this change cannot be due only to refractive index but to the dispersion. Consequently, one should consider not only the real part of the refractive index but also the dispersion, positive if possible, towards obtaining the maximum sensitivity. In view that metallic oxides typically do not show dispersion curves with a positive slope, perhaps the answer to this limitation is the application of synthetic materials or metamaterials. Moreover, there is another research line that should not be underestimated, which is the fabrication of LMR based sensors whose substrate refractive index is similar to the outer medium refractive index, which permits to obtain sensitivities of more than 1 million nm/RIU [11], something that could be achieved also with planar waveguides.

Finally, a last question to consider in the results is the depth of the resonance. It is clear that in Figs. 6 and 8 the LMR tends to fade at longer wavelengths with SnO_2 and ITO respectively, whereas for the CuO coated coverslips the LMR even increases in depth. It is well known that the resonance depth is related to the imaginary part of the refractive index in such a way that there is an optimal case where a maximum depth is achieved [20]. This is explained with the phase matching condition [19,34] (i.e. the equality between a waveguide mode and the lossy mode guided in the nanocoating in the case of a single-mode waveguide or the similarity between the waveguides modes and the lossy mode guided in the nanocoating in the case of a multimode waveguide). In view of the results of Fig. 5, the progressive fading of the LMR at higher wavelengths in the SnO_2 coated coverslip is easily explained by the fact that the imaginary part tends to zero, which leads to a reduction of the resonance depth. For the ITO coating, the imaginary part increases as a function of wavelength, which indicates that we are moving out of the phase matching condition but in opposite direction, towards high values of the imaginary

Optics EXPRESS

part, whereas for the CuO coated coverslip there is a progressive decrease of the imaginary part but it never reaches the zero value in the range from 400 to 1000 nm. In view that the LMR depth increases in Fig. 7 as a function of wavelength, this indicates the possibility that the we are closer to the phase matching condition with the progressive reduction of the imaginary part.

4. Conclusions

The lateral incidence of light in nanocoated coverslips has been used successfully for generating both TE and TM lossy mode resonances (LMRs). Different materials have been explored: SnO_2, CuO and ITO, for the sake of comparing the role of the material in terms of sensitivity to refractive index. Several conclusions could be extracted. The first one is that a material with a higher refractive index permits to obtain the LMR with a thinner coating. In terms of sensitivity to refractive index, it was proved that a higher refractive index leads to a higher sensitivity. By comparing LMRs located at the same wavelength and obtained with different materials, ITO and CuO, it was proved that on average the sensitivity improvement obtained with CuO, with a higher refractive index, was 21.5%. In addition to this improvement, other components such as a location of the wavelength in the optical spectrum of the LMR or the dispersion must also be considered. Regarding the LMR wavelength, it was proved that SnO_2, with a refractive index that on average is about 0.35 units lower that CuO, shows a 24% sensitivity increase compared to CuO in TM polarization and a 17% sensitivity increase in TE polarization. This is explained by the location at higher wavelengths of the SnO_2 resonances analyzed in this work, which demonstrates that the wavelength is a more relevant parameter than the coating refractive index. Regarding the depth of the resonance, it is also clear that the three materials behave differently. The LMR depth increases as a function of wavelength for CuO coated coverslips while decreases for ITO and SnO_2. This fading effect has also been observed in [23] for the first LMR, the most sensitive one, and CuO is the first material that solves this issue, which is also shown in this article as a new material that can be used for generating LMRs. In view of these results, CuO has a great potential in sensors based on this type of phenomenon.

All this indicates the versatility of this optical platform, where by changing the coating materials, or the operating wavelength it is possible to obtain LMRs with different properties. The ability to operate with different materials opens the path to develop chemical, biological or environmental sensors where these materials, or others that satisfy the conditions for LMR generation, can be applied. Moreover, the development of micropatterns on the thin-film is much easier to develop in a slab than in a cylindrical geometry structure like optical fiber Consequently, the last advances of lithography can be applied more easily to this structure, while a wide the range of materials for developing the planar waveguide is available.

Funding

Agencia Estatal de Investigación; European Regional Development Fund (TEC2016-78047-R).

Disclosures

The authors declare no conflicts of interest.

References

1. P. Sanchez, C. R. Zamarreño, M. Hernaez, I. R. Matias, and F. J. Arregui, "Optical fiber refractometers based on Lossy Mode Resonances by means of SnO2 sputtered coatings," Sens. Actuators, B **202**, 154–159 (2014).
2. I. Del Villar, C. R. Zamarreño, M. Hernaez, F. J. Arregui, and I. R. Matias, "Lossy mode resonance generation with indium-tin-oxide-coated optical fibers for sensing applications," J. Lightwave Technol. **28**(1), 111–117 (2010).
3. C. R. Zamarreño, M. Hernáez, I. Del Villar, I. R. Matías, and F. J. Arregui, "Optical fiber pH sensor based on lossy-mode resonances by means of thin polymeric coatings," Sens. Actuators, B **155**(1), 290–297 (2011).

Optics EXPRESS

4. S. P. Usha, S. K. Mishra, and B. D. Gupta, "Fiber optic hydrogen sulfide gas sensors utilizing ZnO thin film/ZnO nanoparticles: A comparison of surface plasmon resonance and lossy mode resonance," Sens. Actuators, B **218**, 196–204 (2015).
5. K. Kosiel, M. Koba, M. Masiewicz, and M. Śmietana, "Tailoring properties of lossy-mode resonance optical fiber sensors with atomic layer deposition technique," Opt. Laser Technol. **102**, 213–221 (2018).
6. D. Tiwari, K. Mullaney, S. Korposh, S. W. James, S. W. Lee, and R. P. Tatam, "An ammonia sensor based on Lossy Mode Resonances on a tapered optical fibre coated with porphyrin-incorporated titanium dioxide," Sens. Actuators, B **242**, 645–652 (2017).
7. I. Del Villar, F. J. Arregui, C. R. Zamarreño, J. M. Corres, C. Bariain, J. Goicoechea, C. Elosua, M. Hernaez, P. J. Rivero, A. B. Socorro, A. Urrutia, P. Sanchez, P. Zubiate, D. Lopez, N. De Acha, J. Ascorbe, and I. R. Matias, "Optical sensors based on lossy-mode resonances," Sens. Actuators, B **240**, 174–185 (2017).
8. A. Andreev, B. Pantchev, P. Danesh, B. Zafirova, E. Karakoleva, E. Vlaikova, and E. Alipieva, "A refractometric sensor using index-sensitive mode resonance between single-mode fiber and thin film amorphous silicon waveguide," Sens. Actuators, B **106**(1), 484–488 (2005).
9. A. T. Andreev, B. S. Zafirova, E. I. Karakoleva, A. O. Dikovska, and P. A. Atanasov, "Highly sensitive refractometers based on a side-polished single-mode fibre coupled with a metal oxide thin-film planar waveguide," IEE Proc.-J: Optoelectron. **10**(3), 035303 (2008).
10. F. J. Arregui, I. Del Villar, C. R. Zamarreño, P. Zubiate, and I. R. Matias, "Giant Sensitivity of Optical Fiber Sensors by means of Lossy Mode Resonance," Sens. Actuators, B **232**, 660–665 (2016).
11. A. Ozcariz, C. R. Zamarreño, P. Zubiate, and F. J. Arregui, "Is there a frontier in sensitivity with Lossy mode resonance (LMR) based refractometers?" Sci. Rep. **7**(1), 10280 (2017).
12. C. R. Zamarreño, M. Hernaez, I. Del Villar, I. R. Matias, and F. J. Arregui, "Tunable humidity sensor based on ITO-coated optical fiber," Sens. Actuators, B **146**(1), 414–417 (2010).
13. F. Chiavaioli, P. Zubiate, I. Del Villar, C. R. Zamarren, A. Giannetti, S. Tombelli, C. Trono, F. J. Arregui, I. R. Matias, and F. Baldini, "Femtomolar Detection by Nanocoated Fiber Label-Free Biosensors," ACS Sens. **3**(5), 936–943 (2018).
14. S. K. Mishra, S. Rani, and B. D. Gupta, "Surface plasmon resonance based fiber optic hydrogen sulphide gas sensor utilizing nickel oxide doped ITO thin film," Sens. Actuators, B **195**, 215–222 (2014).
15. M. Śmietana, M. Sobaszek, B. Michalak, P. Niedziałkowski, W. Białobrzeska, M. Koba, P. Sezemsky, V. Stranak, J. Karczewski, T. Ossowski, and R. Bogdanowicz, "Optical Monitoring of Electrochemical Processes with ITO-Based Lossy-Mode Resonance Optical Fiber Sensor Applied as an Electrode," J. Lightwave Technol. **36**(4), 954–960 (2018).
16. J. M. Corres, J. Ascorbe, F. J. Arregui, and I. R. Matias, "Tunable electro-optic wavelength filter based on lossy-guided mode resonances," Opt. Express **21**(25), 31668–31677 (2013).
17. T. E. Batchman and Glen M. McWright, "Mode Coupling Between Dielectric and semiconductor planar waveguides," IEEE J. Quantum Electron. **18**(4), 782–788 (1982).
18. G. M. McWright, T. E. Batchman, and M. S. Stanziano, "Measurement and analysis of periodic coupling in silicon-clad planar waveguides," IEEE Trans. Microwave Theory Tech. **30**(10), 1753–1759 (1982).
19. M. Marciniak, J. Grzegorzewski, and M. Szustakowski, "Analysis of lossy mode cut-off conditions in planar waveguides with semiconductor guiding layer," IEE Proc. J Optoelectron. **140**(4), 247–252 (1993).
20. I. Del Villar, M. Hernaez, C. R. Zamarreño, P. Sánchez, C. Fernández-Valdivielso, F. J. Arregui, and I. R. Matias, "Design rules for lossy mode resonance based sensors," Appl. Opt. **51**(19), 4298–4307 (2012).
21. F. Chiavaioli, C. A. J. Gouveia, P. A. S. Jorge, and F. Baldini, "Towards a uniform metrological assessment of grating-based optical fiber sensors: From refractometers to biosensors," Biosensors **7**(4), 23 (2017).
22. I. Del Villar, C. R. Zamarreño, P. Sanchez, M. Hernaez, C. F. Valdivielso, F. J. Arregui, and I. R. Matias, "Generation of lossy mode resonances by deposition of high-refractive-index coatings on uncladded multimode optical fibers," J. Opt. **12**(9), 095503 (2010).
23. O. Fuentes, J. M. Corres, I. R. Matias, and I. Del Villar, "Generation of Lossy Mode Resonances in Planar Waveguides Toward Development of Humidity Sensors," J. Lightwave Technol. **37**(10), 2300–2306 (2019).
24. O. Fuentes, I. Del Villar, J. M. Corres, and I. R. Matias, "Lossy mode resonance sensors based on lateral light incidence in nanocoated planar waveguides," Sci. Rep. **9**(1), 8882 (2019).
25. P. Zubiate, A. Urrutia, C. R. Zamarreño, J. Egea-Urra, J. Fernández-Irigoyen, A. Giannetti, F. Baldini, S. Díaz, I. R. Matias, F. J. Arregui, E. Santamaría, F. Chiavaioli, and I. Del Villar, "Fiber-based early diagnosis of venous thromboembolic disease by label-free D-dimer detection," *Biosens. Bioelectron.* X In press (2019).
26. M. Rubin, "Optical properties of soda lime silica glasses," Sol. Energy Mater. **12**(4), 275–288 (1985).
27. N. Sultanova, S. Kasarova, and I. Nikolov, "Dispersion Properties of Optical Polymers," *Acta Phys. Pol., A* **116**(4), 585–587 (2009).
28. I. Del Villar, P. Zubiate, C. R. Zamarreño, F. J. Arregui, and I. R. Matias, "Optimization in nanocoated D-shaped optical fiber sensors," Opt. Express **25**(10), 10743 (2017).
29. V. F. Drobny and L. Pulfrey, "Properties of reactively-sputtered copper oxide thin films," Thin Solid Films **61**(1), 89–98 (1979).
30. I. Del Villar, J. M. Corres, F. J. Arregui, C. R. Zamarreño, C. Bariain, J. Goicoechea, C. Elosua, M. Hernaez, P. J. Rivero, A. B. Socorro, A. Urrutia, P. Sanchez, P. Zubiate, D. Lopez, N. De Acha, J. Ascorbe, and I. R. Matias, "Optical sensors based on lossy-mode resonances," Sens. Actuators, B **240**, 174–185 (2017).

Optics EXPRESS

31. X. Shu, L. Zhang, and I. Bennion, "Fabrication and characterisation of ultra-long-period fibre gratings," Opt. Commun. **203**(3-6), 277–281 (2002).
32. F. Chiavaioli, F. Baldini, S. Tombelli, C. Trono, and A. Giannetti, "Biosensing with optical fiber gratings," Nanophotonics **6**(4), 663–679 (2017).
33. F. J. Arregui, I. Del Villar, C. R. Zamarreño, P. Zubiate, and I. R. Matias, "Giant sensitivity of optical fiber sensors by means of lossy mode resonance," Sens. Actuators, B **232**, 660–665 (2016).
34. D. Kaur, V. K. Sharma, and A. Kapoor, "High sensitivity lossy mode resonance sensors," Sens. Actuators, B **198**, 366–376 (2014).